

## DESIGN OF A BUNCHING SYSTEM FOR A HIGH-INTENSITY ELECTRON LINAC \*

Roger H. Miller, Stanford Linear Accelerator Center  
and

Charles H. Kim and Frank B. Selph  
Accelerator and Fusion Research Division, Lawrence Berkeley Laboratory  
University of California, Berkeley, California 94720

### Abstract

The Advanced Light Source, under construction at the Lawrence Berkeley Laboratory, will use a 50 MeV, 3 GHz linac as preinjector. The linac will operate in two modes—a single-bunch mode of 4 nC/pulse and a 100 - 150 nanosecond multibunch mode with 125 mA average current. In both modes an rms momentum spread of  $<0.3\%$  is needed. The linac injection system consists of a high-intensity gun, followed by two subharmonic bunchers (one of  $1/24$ th, and the other of  $1/6$ th the linac frequency), an S-band buncher at the linac frequency and the first few cavities of the linac (the capture section). The beam experiences strong space-charge forces and nonlinearities which cause emittance growth. Expected performance is analyzed with computer simulations.

### Introduction

The Advanced Light Source (ALS)—a national user facility at the Lawrence Berkeley Laboratory<sup>1</sup>—has been under construction since October 1987. It employs a low emittance electron storage ring which is optimized for insertion devices. The facility is expected to serve several hundred users at a time when fully operational, including 48 bending-magnet beam lines.

The injector complex for the storage ring will consist of a bunching system, a 50 MeV disk-loaded traveling-wave linac, and a 1 Hz, 1.5 GeV booster synchrotron.<sup>2,3</sup> The injector complex must be very reliable and must have the capability of filling the storage ring rapidly with minimum interference to users. We have followed a conservative design practice, using only well-proven technologies, to ensure that these design requirements are met.

The bunching system described in this report forms part of the low energy transport line between the gun and the linac. Its purpose is to compress the gun output current and generate high intensity

(several nC) electron pulses with a short duration (20 ps) that must be injected into the linac rf bucket such that the resulting energy spread at the linac exit is within the acceptance of the booster ( $\pm 1\%$ ).

We considered two possible approaches in designing the ALS bunching system: (1) the subharmonic bunching approach; and (2) the photocathode rf gun approach. The subharmonic bunching system was adopted because it is reliable and the technology is mature.

Space-charge effects and nonlinearities are very strong in the bunching system and tend to cause longitudinal and transverse emittance growth. We have simulated the expected performance of the bunching system using the PARMELA<sup>4</sup> code.

### Description of the ALS Bunching System

A schematic diagram of the bunching system is shown in Fig. 1. The electron gun is similar to the one used by SLC; it will be capable of producing 2-4 A of peak current at a nominal energy of 120 keV with a normalized rms emittance of  $8\pi$  mm-mrad. The gun current can be pulsed for a minimum duration of 2.5 ns, at the maximum rate of 125 MHz. We plan to use at most 18 consecutive micro-pulses ( $<150$  ns) at a time. This is suitable for single-turn injection into the booster. A drift region of 100 cm between the gun and the 125 MHz subharmonic buncher is necessary for beam instrumentation and for bucking the solenoidal focusing field at the gun.

The 125 MHz subharmonic buncher is a reentrant resonant cavity excited in the TEM mode. It captures 2.5-ns gun pulses in  $\pm 60^\circ$  of the sine-wave bunching field. The 500 MHz buncher is of similar design but smaller in size. Pulse compression by the two subharmonic bunchers is expected to be about a factor of 10.

The S-band buncher is a traveling wave structure with a wave

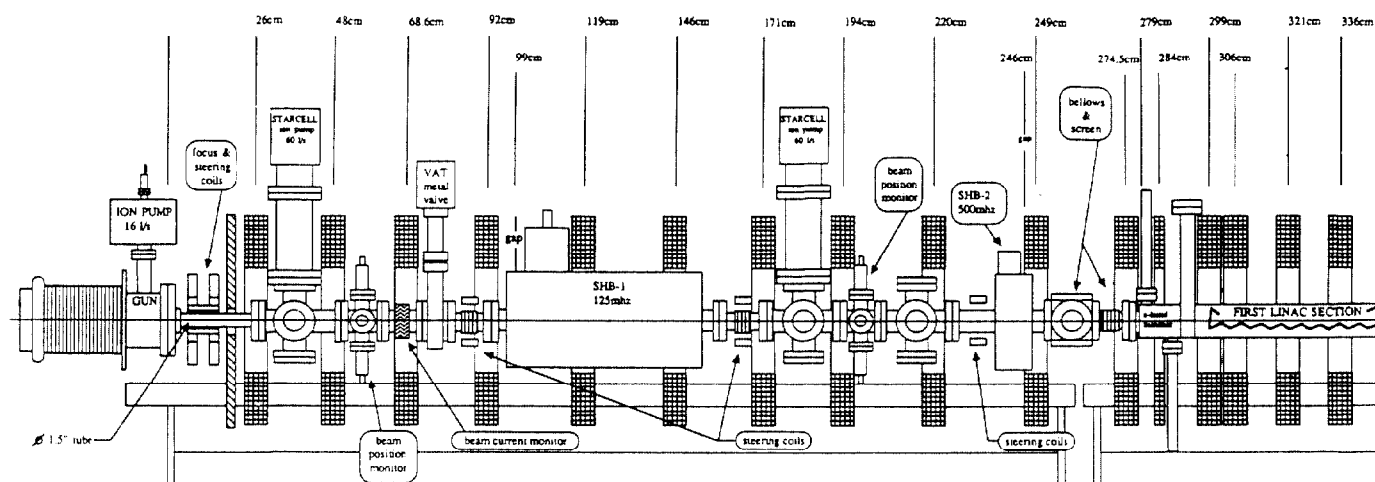


Figure 1. The ALS bunching system.

\*This work is supported by the Office of Basic Energy Science of the U.S. Department of Energy under Contract No. DE-AC03-76SF00098

velocity,  $\beta_w = 0.75c$ . This buncher also accelerates electrons for efficient capture in the linac. The capture section is the first 15 cm of the linac proper, which is a disk-loaded traveling-wave structure with  $\beta_w = c$ .

Solenoidal focusing is used to maintain the beam radius at about 7 mm throughout the bunching system.

### Beam Dynamics Study

#### Model

PARMELA<sup>4</sup> works with a few hundred to a thousand macro-particles in a cylindrically symmetric geometry. The space-charge forces are calculated in the beam frame, where the self-forces are assumed to be purely electrostatic. The electric fields are calculated in the following manner: an  $r$ - $z$  mesh ( $\leq 41$  points along  $z$ ,  $\leq 11$  points along  $r$ ) is set up, just large enough to cover the electron bunch (but not necessarily cover all the vacuum region between the beam and the wall); values of electric fields at points along  $r$ , at  $z=0$ , due to a unit charge at a mesh point, are calculated for every mesh point, using the formula for a charged ring. This field table is stored and used repeatedly as a Green's function to calculate the actual electric fields. The code adjusts the size of the mesh automatically when the size of the electron bunch changes more than a certain user-specified factor (either by a pulse compression or by a Lorentz decontraction due to acceleration). The Green's functions are recalculated after each remeshing.

We found that significant errors can be introduced in the space-charge calculation if the aspect ratio of the mesh becomes too large or too small. We overcame this difficulty by adopting a dual meshing system in which the particle distribution is allowed to have a larger number ( $\leq 201$ ) of  $z$ -mesh points of the same size as the space-charge meshes. For a short bunch (length/radius  $\leq 60$ ) the two mesh systems are identical. For a long bunch, the space-charge mesh has fewer points than the particle mesh: space-charge forces by particles far away ( $\geq 60 \times$  beam radius) are small, and neglected in favor of keeping the mesh aspect ratio close to 1.

The 125 MHz and the 500 MHz subharmonic bunchers are modeled as having zero gaps with sinusoidal accelerating fields. The S-band buncher and the linac rf fields are evaluated from the spatial

harmonics whose coefficients are either calculated by another method or by matching the boundary conditions at the radius of the orifice of the structure.

We present here some typical 4 nC runs with initial bunch length of 2 ns. These runs are made on an IBM PS/2 Model 80 personal computer, and each run requires about 30 minutes for the 315 cm bunching system. The first run requires somewhat longer time to calculate the Green's functions (that are then stored and reused for the subsequent optimization runs).

#### Longitudinal dynamics

Fig. 2 represents the evolution of the particle distribution in  $(\beta\gamma)_z$ - $z$  phase space, and  $r$ - $z$  configuration space, for a single bunch as it moves through the two subharmonic bunchers. Each cluster of points represents a picture of the electrons at a given time. The time intervals between clusters are not uniform. End-erosions due to the longitudinal space-charge forces can be clearly seen for  $z < 100$  cm. Also notice the velocity modulations generated by the 125 MHz buncher ( $z=100$ cm) and the 500 MHz buncher ( $z=240$  cm).

Velocity is a nonlinear function of  $z$  because (1) the bunching field is a sinusoidal function of time and (2) the velocity is a nonlinear function of energy. These nonlinearities cause the particles near the front of the pulse to bunch faster than the rest, forming a dense core of electrons with strong repulsive space-charge forces; particles near the edge of this core are strongly affected. A similar phenomenon was previously reported in Ref. [6].

Figure 3 shows the evolution of the particle distribution in the S-band buncher and the capture section. The electrons enter the S-band buncher with a rather high phase spread of  $200^\circ$ —too large for the linac. Furthermore, the electron energy of 120 keV is too low for the linac, because the phase slippage in the first several cavities would be too large. The tasks of the S-band buncher, then, are to further compress the beam longitudinally while accelerating it. Compression is accomplished by adjusting the initial rf phase spread to lie between  $-100^\circ$  and  $100^\circ$ . Acceleration takes place when rf waves overtake the electrons and the center rf phase gradually increases to  $90^\circ$  at the end of the S-band buncher. The accelerating gradient in the S-band buncher is only 3.5 MV/m so that the electrons have enough time to bunch.

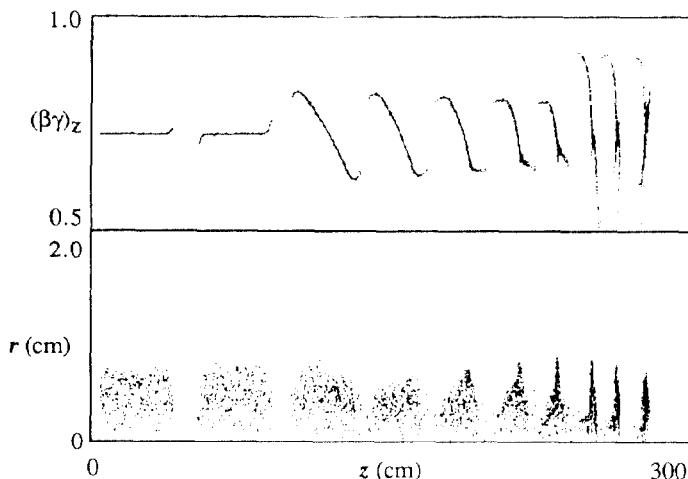


Figure 2. PARMELA simulation of the evolution of particle distribution in  $(\beta\gamma)_z$ - $z$  space, and  $r$ - $z$  space in the subharmonic buncher region

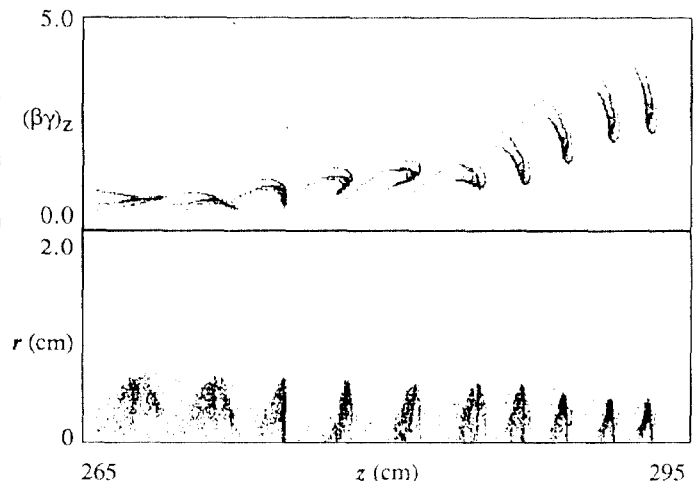


Figure 3. The same as in Fig. 2 for the S-band buncher and the capture region.

Final compression of the pulse (by a factor of 3) occurs in the capture section in a similar way to that in the S-band buncher. Electrons enter the linac proper with an rf phase between  $-30^\circ$  and  $+30^\circ$  and a kinetic energy between 230 keV and 400 keV. The gradient in the linac is 15 MV/m; electrons become highly relativistic in the first few cavities, and the phase is locked to about  $90^\circ \pm 10^\circ$  for the rest of the linac.

### Transverse Dynamics

The rf fields in the S-band buncher and in the linac have radial electric field components that vary almost linearly with radius and sinusoidally with time. The rf fields and the space-charge forces are defocusing forces that are compensated by axial magnetic fields, which are constant in time. The radial rf electric field thus acts differently on the different longitudinal segments of the electron pulse. When the distribution is integrated over the longitudinal coordinate, the effective transverse emittance is increased.<sup>6</sup> The normalized rms emittance is plotted in Fig. 4 as a function of  $z$ . The most significant emittance growth occurs in the S-band buncher, as expected. Emittance growth is negligible in the linac proper because the bunch length is very short ( $4\sigma \sim 20^\circ$ ) and appears to oscillate around  $40 \pi$  mm-mrad.

The scatter plots in Figs. 5 (a), (b), and (c) show typical particle distributions in horizontal phase space at three  $z$  locations. Initially ( $z=0$  cm), electrons are loaded uniformly in a square box in phase space (Fig. 5(a)). The butterfly-shape distribution in Fig. 5(b) is in the middle of the S-band buncher. The halo in Fig. 5(c) oscillates around the denser core of the distribution; the beam is less intense at the head and tail and undergoes envelope oscillations around the Brillouin equilibrium radius.

### Summary

We have designed a bunching system for the LBL ALS facility based on proven technology using subharmonic bunchers. Our simulation results using PARMELA show that, at the end of the 50 MeV linac, more than 80% of 4 nC are within the 1% energy spread required for the booster. The transverse emittance growth is significant but saturates at around  $40 \pi$  mm-mrad normalized rms, which is comfortably below the value assumed in our earlier design.

### Acknowledgment

The authors wish to thank J. Giugli, C. C. Lo, B. Taylor and B. Woo for their valuable helps. Colleagues at the ALS Accelerator Systems Group, especially M. Zisman, are acknowledged for critically reading the manuscript.

### References

- 1 "1-2 GeV Synchrotron Radiation Source conceptual Design Report", LBL Report, PUB-5172 Rev., July, 1986.
- 2 F. Selph, A. Jackson, and M. Zisman, Proceedings of the 1987 IEEE Particle Accelerator Conference, p. 446.
- 3 M. S. Zisman, LBL Report, LBL-24963 March (1988).
- 4 L. Young, private communication.
- 5 H. Hanerfeld, W. B. Herrmannsfeldt, M. B. James and R. H. Miller, IEEE Trans. Nucl. Science, Vol. NS-32, 2510 (1985).
- 6 K. -J. Kim, private communication.

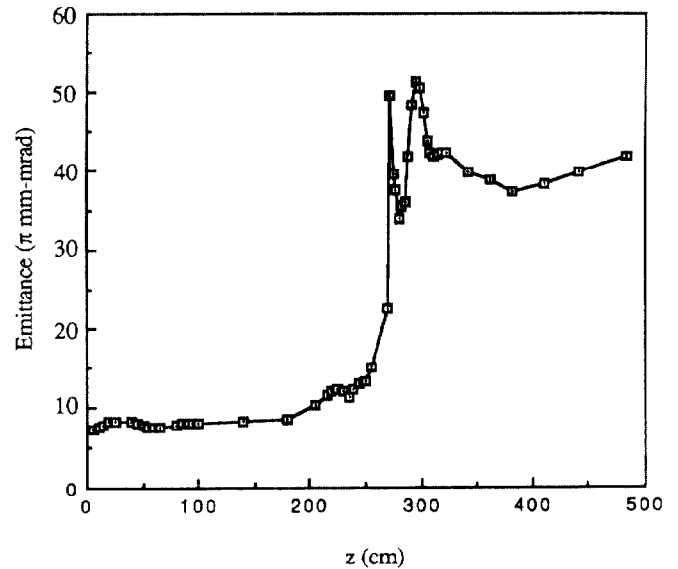


Figure 4. Normalized rms emittance,  $\epsilon_x$ , of the horizontal plane as a function of  $z$ .  $\epsilon_x = (\langle x^2 \rangle \langle (\beta\gamma)_x^2 \rangle - \langle x (\beta\gamma)_x \rangle^2)^{1/2}$

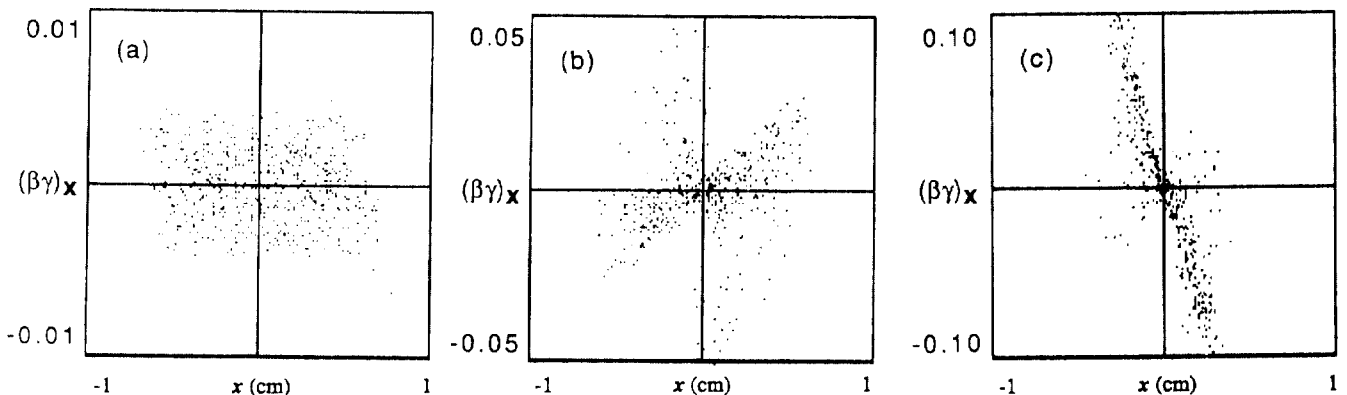


Figure 5. Evolution of particle distribution in  $(\beta\gamma)_x - x$  space at (a) initial loading of particles,  $z=5$  cm; (b) in the middle of the S-band buncher;  $z=275$  cm, and (c) after the capture in the linac;  $z=295$  cm